

UC Davis

UC Davis Previously Published Works

Title

Multicopper manganese oxidase accessory proteins bind Cu and heme

Permalink

<https://escholarship.org/uc/item/83q8q4fd>

Journal

Biochimica et Biophysica Acta, 1854(12)

ISSN

0006-3002

Authors

Butterfield, Cristina N
Tao, Lizhi
Chacón, Kelly N
[et al.](#)

Publication Date

2015-12-01

DOI

10.1016/j.bbapap.2015.08.012

Peer reviewed



Multicopper manganese oxidase accessory proteins bind Cu and heme



Cristina N. Butterfield^{a,1}, Lizhi Tao^b, Kelly N. Chacón^{a,2}, Thomas G. Spiro^c, Ninian J. Blackburn^a, William H. Casey^d, R. David Britt^b, Bradley M. Tebo^{a,*}

^a Division of Environmental and Biomolecular Systems, Institute of Environmental Health, Oregon Health & Science University, Portland, OR 97239, United States

^b Department of Chemistry, University of California, Davis, CA 95616, United States

^c Department of Chemistry, University of Washington, Seattle, WA 98195, United States

^d Department of Geology, University of California, Davis, CA 95616, United States

ARTICLE INFO

Article history:

Received 1 July 2015

Received in revised form 24 August 2015

Accepted 27 August 2015

Available online 29 August 2015

Keywords:

Multicopper oxidase

Metallo-subunit

Electron paramagnetic resonance spectroscopy

Type 2 copper

X-ray absorption spectroscopy

Protein oligomerization

ABSTRACT

Multicopper oxidases (MCOs) catalyze the oxidation of a diverse group of metal ions and organic substrates by successive single-electron transfers to O₂ via four bound Cu ions. MnxG, which catalyzes MnO₂ mineralization by oxidizing both Mn(II) and Mn(III), is unique among multicopper oxidases in that it carries out two energetically distinct electron transfers and is tightly bound to accessory proteins. There are two of these, MnxE and MnxF, both approximately 12 kDa. Although their sequences are similar to those found in the genomes of several Mn-oxidizing *Bacillus* species, they are dissimilar to those of proteins with known function. Here, MnxE and MnxF are co-expressed independent of MnxG and are found to oligomerize into a higher order stoichiometry, likely a hexamer. They bind copper and heme, which have been characterized by electron paramagnetic resonance (EPR), X-ray absorption spectroscopy (XAS), and UV–visible (UV–vis) spectrophotometry. Cu is found in two distinct type 2 (T2) copper centers, one of which appears to be novel; heme is bound as a low-spin species, implying coordination by two axial ligands. MnxE and MnxF do not oxidize Mn in the absence of MnxG and are the first accessory proteins to be required by an MCO. This may indicate that Cu and heme play roles in electron transfer and/or Cu trafficking.

© 2015 Elsevier B.V. All rights reserved.

1. Introduction

Many metalloproteins that conduct electron transfer and redox processes are composed of oligomeric protein complexes whose subunits play essential roles in function. MoFe-protein from nitrogenase [1–3], β and γ carbonic anhydrase [4–6], ammonia and particulate methane monooxygenase [7,8], ribonucleotide reductase [9], and cytochrome c oxidase [10] are all examples of multi-subunit proteins whose catalytic functions rely on the redox mechanisms of their metalcenters. Elucidating these mechanisms begins with the characterization of individual metal binding centers in isolated subunits.

Multicopper oxidases (MCOs), on the other hand, have previously only been isolated as monomers and homopolymers. MCOs catalyze

the oxidation of a variety of substrates, including phenolic compounds and metals, as well as the reduction of O₂ to H₂O [11,12]. They facilitate numerous physiological functions including morphogenesis, stress defense, and lignin degradation [11]. All MCOs have at least four canonical Cu atoms bound within three spectroscopically distinct centers. The three spectroscopically distinct centers are a type 1 center, which is comprised of one S(Cys), one S(Met), and two N(His), a type 2 center with three N(His) ligands, and a type 3 binuclear center which coordinates Cu using two N(His) ligands per Cu atom. Electron transfer commences at the substrate site, proximal to the type 1 Cu. A network of peptide bonds guide electron flow to a trinuclear cluster, composed of one type 2 Cu and a type 3 binuclear center, which are ~9 Å from the type 1 Cu [13]. The final electron acceptor, O₂, binds at the trinuclear center, forming two water molecules after four successive one-electron transfers. MCOs are arranged in two, three, or six domain structures, with the Cu centers being formed by ligands across protein domains. Until the discovery of the Mnx complex in the marine *Bacillus* species PL-12 [14], MCOs were heterologously expressed as single gene products and no MCO required additional subunits for function.

Mnx is a multi-protein complex that is located on the outer spore surface and has been shown to catalyze Mn(II) oxidation and form MnO₂ mineral [15,16]. While the role MnO₂ formation plays in spore function is unclear, a large cellular energy investment is made in order to produce Mnx. The expression of soluble and active Mn oxidase

Abbreviations: MCO, multicopper oxidase; EPR, electron paramagnetic resonance; EXAFS, extended X-ray absorption spectroscopy; UV–vis, UV visible; SDS-PAGE, sodium dodecyl sulfate polyacrylamide gel electrophoresis; ICP-OES, inductively coupled plasma-optical emission spectrometry; MnxEF, refers the product of the co-expression of genes *mnxE* and *mnxF*; MnxEF3, refers to the H21A, H80A, and H82A modified protein.

* Corresponding author.

E-mail address: tebob@ohsu.edu (B.M. Tebo).

¹ Present affiliation: Department of Earth and Planetary Science, University of California, Berkeley, CA 94720, United States.

² Present affiliation: Reed College, Department of Chemistry, Portland, OR 97202, United States.

requires the co-expression of at least three genes on the *mnx* gene cluster: *mnxG*, the multicopper oxidase (MCO), and *mnxE* and *mnxF*, small proteins of unknown function [14]. The three proteins co-purify into a complex of roughly 230 kDa in size, and reported to bind anywhere from 6.4–15 Cu atoms per protein complex [14,17]. Like all MCOs, MnxG contains a type 1 Cu and carries out substrate oxidation, but since no other MCO requires the co-expression of subunits, the specific roles of MnxE and MnxF have been unclear.

Characterizing the metal binding features of the Mnx complex subunits is essential to piecing together its mechanism. The MnxE and MnxF subunits are small, ~12 kDa proteins and are well-conserved among the Mn oxidizing *Bacillus* spp. that have been sequenced, yet they do not contain any conserved domains from which one could predict function. MnxF is reported to possess a potential Cu-binding site [16]; there are several histidine and cysteine residues in MnxE and MnxF that could potentially bind Cu. Importantly, the MCO MnxG cannot be expressed in a soluble active form if it is not synthesized with MnxE and MnxF in the cell, but the latter can be separately purified as an oligomer, MnxEF. We made site-directed mutations at three potential Cu binding sites and utilized electron paramagnetic resonance (EPR), X-ray absorption spectroscopy (XAS), and UV–visible spectrophotometry (UV–vis) to characterize wild type and mutant MnxEF and the complete MnxG(EF) complex. Herein, we characterize the metal cofactors associated with the MnxEF accessory proteins, which provides insights into their possible function in the larger MnxEFG complex and implicates their role as integral metal-facilitated redox partners that contribute to electron transfer during Mn oxidation.

2. Methods

2.1. Alignments

Alignments were carried out with MUSCLE with default parameters on the following URL <http://www.ebi.ac.uk/Tools/msa/muscle/> [18,19] with NCBI accession numbers MnxE PL-12 ABP68888, MB-7 ABP68897, and SG-1 EDL64242 and MnxF PL-12 ABP68889, MB-7 ABP68898, and SG-1 EDL64243.

2.2. Cloning and mutagenesis

mnxE and *mnxF* (NCBI accession EF158106) were amplified from *Bacillus* sp. PL-12 (Taxonomy ID: 161537) genomic DNA by the following primers: Fwd 5'-**CCGCGGTATGCATGACTCGCCATT**-3' and Rvs 5'-**GTCGACATAGTCTTCGAGCTTCG**-3'. *mnxDEFG* were amplified by the following primers: Fwd 5'-**CCGCGGTATGCATTCGGATTATTGAAAAATTGT**-3' and Rvs 5'-**GTCGACTGCCTTTCTTCATTGTCCACC**-3'. These two amplicons were ligated into pJet1.2 (Thermo) entry vectors, then cloned by restriction enzyme digestion and ligation into the *Strep*-tag pASK/IBA3plus expression vector using SacII and Sall (sequences in bold). In place of the *mnxF* or *mnxG* stop codon the *Strep*-tag (underlined) was engineered to a linker (italicized) at the C-terminus (***VDLQGDHGLSAW****SHIQFEK*). Single amino acid mutations were generated in the pJet1.2/*mnxDEFG* construct with the Stratagene QuickChange® site-directed mutagenesis kit (Agilent). MnxF H21, 80, and 82 were changed to Ala. Then the *mnxEF* H21/80/82A mutant or *mnxDEFG* H21/80/82A were PCR amplified from the pJet1.2/*mnxDEFG* construct and cloned into an empty pJet1.2 plasmid and moved to the pASK/IBA3plus vector as described above.

2.3. Gene expression, in vivo Cu loading, and protein purification

The resulting constructs were transformed into *Escherichia coli* BL21 (DE3) and grown at 37 °C to an OD₆₀₀ ~ 0.5 in Luria–Bertani (LB) broth containing 0.2 mM CuSO₄, 10 mM Tris–HCl pH 7.5, and 100 mg/l ampicillin. The temperature was then lowered to 17 °C by cooling the culture on ice or in a refrigerated shaker (for *mnxDEFG* expression) or kept at

37 °C (for *mnxEF* expression) and then 0.2 mg/l anhydrotetracycline was added to induce transcription of the *mnx* genes. The cells continued to shake and express for 16–20 h (for *mnxDEFG*) or for 3 h (for *mnxEF*). CuSO₄ was added to a final concentration of 2 mM and the shaking function was stopped for at least 22 h to allow for the microaerobic uptake of Cu ions into the *E. coli* cytoplasm as described in Durao et al. [20]. This Cu loading step was omitted during the protein preparation to obtain the “partially loaded” protein.

The cells were harvested by centrifugation 5000 ×g 4 °C 10 min, suspended in *Strep*-Tactin wash buffer (100 mM Tris pH 8.0, 150 mM NaCl) amended with 1 mM CuSO₄ and an EDTA-Free SIGMAFAST™ Protease Inhibitor Cocktail Tablet, and lysed using a sonication microtip for 1 min/ml cell lysate at 40% amplitude with 10 s on/off pulses on ice. The cell debris was pelleted by centrifugation 15,000 ×g 4 °C 30 min and the supernatant was filtered through a 0.4 μm pore PVDF filter. The clarified lysate was then added to 1 ml (for MnxEF protein) or 5 ml (for MnxDEFG protein) column volume (CV) of *Strep*-Tactin Superflow Plus (Qiagen). By peristaltic pump (~1 ml/min flow rate), the unbound protein fraction was removed and the resin was washed with 20 CV *Strep*-Tactin wash buffer. The protein was eluted with 5 CV wash buffer plus 2.5 mM D-Desthiobiotin and the column was regenerated with 15 CV wash buffer plus 1 mM 2-(4-hydroxyphenylazo) benzoic acid. The eluted protein was concentrated to <1.5 ml on 50 kDa (for MnxEF) or 100 kDa (for MnxDEFG) molecular weight cutoff filtration units (Millipore). The protein was then dialyzed in 50 mM Tris–HCl pH 8 and decreasing NaCl concentrations from 150 to 50 mM NaCl and flash frozen with 20% ethylene glycol for future analyses. The protein was quantified by the Thermo Scientific Pierce bicinchoninic acid (BCA) protein assay.

2.4. Mass spectrometry

Purified protein was run on Tris Glycine 4–15% sodium dodecyl sulfate polyacrylamide electrophoresis gel (Bio-Rad) and stained in Imperial protein stain (Pierce). The protein band that migrated to 12 kDa according to the PageRuler™ Unstained Protein Ladder (Thermo) was excised by a clean razor blade and submitted to the Oregon Health & Science University Proteomics Shared Resource Center for analysis with the *Bacillus* sp. PL-12 *mnxE* and *mnxF* triple mutant sequences. Mass spectrometric analysis was performed as previously described in Butterfield et al. 2013 [14].

2.5. UV–visible spectroscopy

The UV–visible spectra were collected on a SpectraMax M2 in a 50 μl 1 cm path length quartz cuvette.

2.6. Electron paramagnetic resonance (EPR) spectrometry

X-band continuous wave electron paramagnetic resonance (CW EPR) spectra were recorded using a Bruker (Billerica, MA) Biospin EleXsys E500 spectrometer equipped with a cylindrical TE011-mode resonator (SHQE-W). Cryogenic temperatures were achieved and controlled using an ESR900 liquid helium cryostat in conjunction with an Oxford Instrument temperature controller (ITC503) and gas flow controller. All CW-EPR data were collected under non-saturation and slow-passage conditions. The spectrometer settings used were as follows: microwave frequency = 9.374 GHz, microwave power = 0.2 mW, conversion time = 40 ms, modulation amplitude = 8 G, and modulation frequency = 100 kHz. EasySpin computational package was used to simulate the EPR data [21].

2.7. Mn oxidation activity assay

Protein was routinely purified to a concentration of about 5–10 μM in 3 ml before concentrating. A small aliquot of purified protein was

diluted into 1 ml 10 mM HEPES pH 7.8 and 50 mM NaCl to a final protein concentration of about 500 nM and 100 μ M MnCl₂ was added. The appearance of brown Mn oxides within 10 min and reactivity with the colorimetric reagent leucoberberlin blue confirmed activity.

2.8. X-ray absorption spectroscopy

A solution of 3 mM Cu-loaded MnxEF was treated with excess dithionite to ensure the cuprous form of the metalloprotein, and was measured as an aqueous glass in 20% ethylene glycol at 10 K. Cu K-edge (8.9 keV) extended X-ray absorption fine structure (EXAFS) and X-ray absorption edge data were collected at the Stanford Synchrotron Radiation Lightsources, on beamline 7–3 with an Si 220 monochromator, in fluorescence mode using a high-count rate Canberra 100-element Ge array detector. A Ni filter and a Soller slit were placed in line with the detector to attenuate the elastic scatter peak. For energy calibration, a Cu foil was placed between the second and third ionization chamber. Four scans of a buffer blank were averaged and subtracted from the raw data to produce a flat pre-edge and remove any residual Ni fluorescence. Data reduction and background subtraction were accomplished using the EXAFSPAK suite [22] and the data was inspected for dropouts and glitches before averaging. The EXCURV program was used for spectral simulations as described previously [23,24].

3. Results

3.1. MnxE and MnxF copurify and oligomerize

The MnxE and MnxF primary sequences are highly conserved among the Mn oxidizing *Bacilli* that have been sequenced (Dick et al. 2008). A previous sequence alignment of MnxE and MnxF identified a region in MnxF with significant similarity to the Cu binding region found in the MCOs, including one His of type 2 and one His of type 3 Cu [16]. We performed a new sequence alignment for the three *Bacillus* spp. MnxE and MnxF to find additional conserved Cu binding ligand candidates (Supplemental Fig. 3). MnxF has exactly three His residues conserved in all three sequenced *Bacillus* spp., H21, H80, and H82, which are attractive contenders for type 2 Cu binding ligands. These three residues were mutated to Ala to probe whether the Cu binding properties of the subunits would be disrupted (see below).

The MnxE and MnxF subunits were co-expressed from a MnxF C-terminal *Strep* tag plasmid and purified on a Streptactin column. A MnxF triple His to Ala mutant was constructed, co-expressed with wtMnxE, and isolated in the same manner. This modified protein was run on SDS PAGE (sodium dodecyl sulfate polyacrylamide gel electrophoresis) and the protein corresponding to 12 kDa mass (Supplemental Fig. 1) was analyzed by mass spectrometry to ensure that both MnxE and MnxF peptides were present and that mutagenesis was successful. Mass spectrometric analysis confirmed the mutagenesis (Supplemental Fig. 2) and identified 108 unique peptides from MnxE (100% coverage) and 67 from MnxF (89% coverage). These results show that even without MnxG present, MnxE and MnxF co-elute in the same fraction when only MnxF contains the affinity tag.

The stoichiometry of the MnxEF subunits in relation to each other and to the MnxG MCO is yet unknown. When *mnxDEFG* is expressed and purified, a large 230 kDa complex is isolated, composed of MnxE (12.2 kDa), MnxF (13.5 kDa), and MnxG (138 kDa) by mass spectrometric analysis [14]. By summation, MnxE and MnxF would have to comprise about 90 kDa of the complex mass, and we have previously surmised that they oligomerize into a hexamer because a soluble protein fraction eluted in gel filtration chromatography at a calculated mass of 77 kDa (data not shown). Thus, for the rest of the discussion, we assume purified MnxEF is in a hexamer (77 kDa) and refer to the MnxEF triple H21/80/82A mutant as MnxEF3.

MnxF mutations H21/80/82A were incorporated in the genes expressed for subunit analysis, *mnxEF*, and for activity analysis in the

Mnx complex, *mnxDEFG*. None of them showed divergence in activity with respect to wild type. MnxEF and MnxEF3 do not oxidize Mn, but when co-expressed with MnxG, both wild type and triple mutant variants oxidize Mn at roughly the same rate (within 10 min, not shown). Thus, MnxF H21, H80, and H82 do not seem to play a significant role in Mn oxidation.

3.2. Cu binding analyses

In a previous study, the best estimate for Cu binding by the Mnx protein complex was a minimum of ten mol Cu per mol protein [17,25]. It is presumed that four Cu atoms reside in the MCO while six or more are yet to be assigned locations and might be in the E and F subunits. These subunits were expressed, purified, and loaded with Cu in a similar manner to the Mnx protein complex. The Cu content analyses of the newly purified MnxEF subunits by inductively coupled plasma-optical emission spectrometry (ICP-OES) (2.6 Cu:1 MnxEF hexamer) and by Cu(II) EPR (2.8 Cu:MnxEF) both yielded a Cu:protein molar ratio of about 3:1, three atoms short of the ten to be accounted for.

The Cu binding site in WT MnxEF was analyzed by X-band (9.374 GHz) CW EPR spectroscopy, as shown in Fig. 1. A typical type 2 Cu ('normal Cu', square planar coordination) signal with hyperfine coupling ($g_{\parallel} \approx 2.215$, $A_{\parallel} \approx 594$ MHz) was observed, which also contributes to the spectrum of WT MnxEFG (red trace in Fig. 1). The remaining features in the WT MnxEFG trace likely arise from Type 1 Cu and Type 2 Cu sites in MnxG but their assignments require further investigation. It should be noted that there is a small, negative g value shift in the MnxEF Type 2 Cu in the complex MnxEFG spectrum, suggesting that the electronic structure of the Cu(II) sites in MnxEF subunit is affected when binding to MnxG.

3.3. Heme binding analysis

Both wtMnxEF and MnxEF3 are orange in color when purified and concentrated whether loaded with Cu or not. Their UV-visible spectra showed an absorbance peak at 412 nm (Fig. 2). Reduction of the protein with dithionite and ascorbate (not shown) did not change the color but

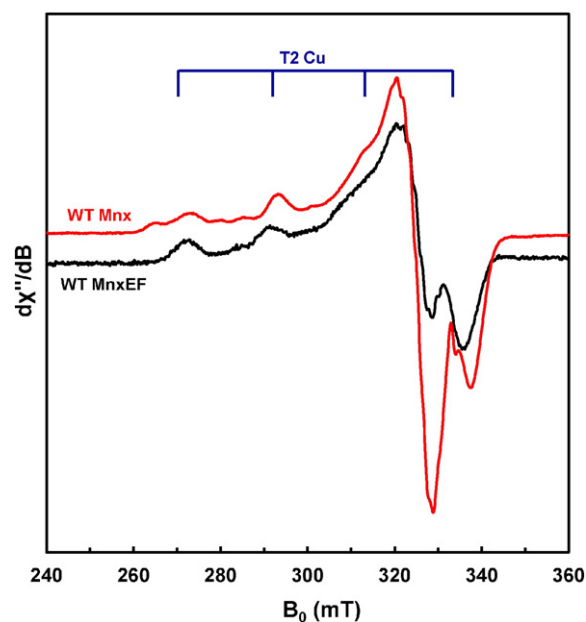


Fig. 1. X-band CW EPR spectra of WT MnxEF (black) and WT MnxEFG complex (red). The samples were analyzed at 60 K and 0.02 mW power. Parameters: microwave frequency: 9.374 GHz, conversion time: 40 ms, modulation amplitude: 8 G, and modulation frequency: 100 kHz. Type 2 Cu peaks were identifiable in the WT MnxEF. WT Mnx protein complex contains multiple Type 2 Cu [17] that mask the contribution of the Type 1 Cu so its peaks cannot be labeled.

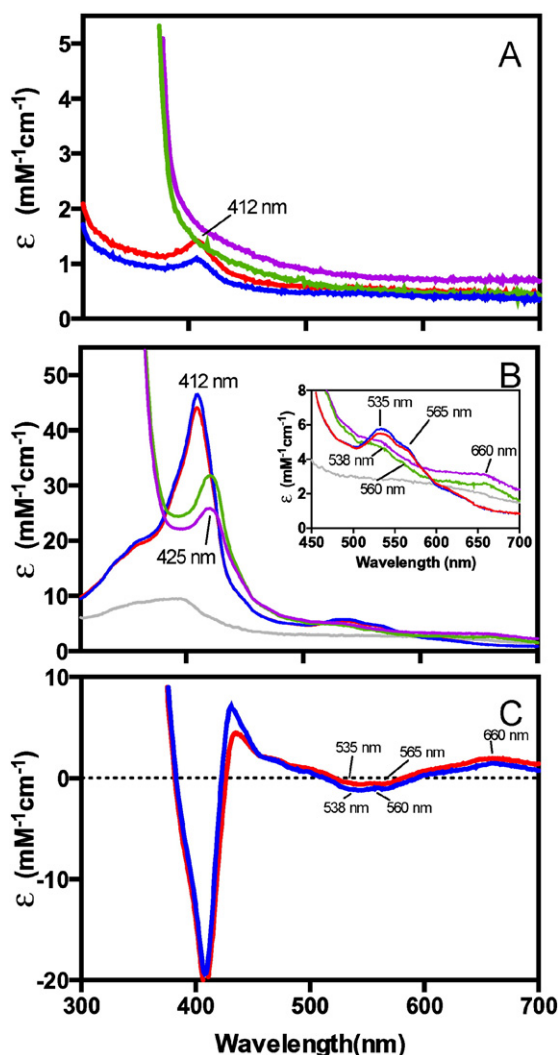


Fig. 2. UV-visible spectra before and after heme loading, and subsequent reduction with dithionite. A. As purified wtMnxEF (blue) and MnxEF H21/80/82A mutant (MnxEF3) (red) contain the same Soret 412 nm peak. Addition of dithionite to wtMnxEF (purple) and MnxEF3 (green) proteins produced a large, broad peak that masks any observable change to the Soret peak. B. The addition of heme to MnxEF and MnxEF3 intensifies the 412 nm peak and visible peaks 538 nm and 565 nm (inset). After reduction of heme-MnxEF (2 \times) and heme-MnxEF3 (2 \times), the Soret band shifts to 424 nm and the visible bands at 535 nm and 660 nm appear (inset). Bovine hemin (0.1 \times gray) is shown for comparison. C. Difference spectra (oxidized subtracted from reduced) of heme loaded wild type MnxEF (blue) and MnxEF3. ϵ = absorbance \times (MnxEF hexamer concentration) $^{-1}$.

did overwhelm the 412 nm peak with an intense, broad peak around 320 nm [26,27]. This ruled out the possibility of the presence of a colored Cu center since a red Cu(II) would have turned clear upon reduction to Cu(I). Bovine hemin was added to wtMnxEF and MnxEF3 and then excess was removed by desalting spin columns and dialysis. The resulting protein was diluted and its spectrum was typical of Fe(III) heme with the Soret band observed at 412 nm and visible bands at 558 nm and 565 nm (Fig. 2). Upon the addition of 10 mM dithionite, the Soret band shifted to 425 nm, while the visible bands shifted to 538 nm and 560 nm, consistent with reduction to Fe(II) heme. The reduced heme concentration was estimated using the extinction coefficient for heme of 120 mM $^{-1}$ cm $^{-1}$ [28]. Before heme loading, the molar ratio heme to protein was 0.009:1 for wtMnxEF and 0.011:1 for MnxEF3. After heme loading, the ratio increased to 0.38:1 for wtMnxEF and 0.36:1 for MnxEF3.

3.4. Cu spectroscopic analyses

wtMnxEF and MnxEF3 samples with varying Cu stoichiometry were prepared. Adding Cu during protein expression resulted in maximum loading of 2.8 Cu/MnxEF and 3 Cu/MnxEF3. When protein was expressed without extra Cu, the Cu content was 1.36 Cu/MnxEF and 0.26 Cu/MnxEF3. These samples were analyzed by X-band (9.38 GHz) CW EPR spectroscopy, as shown in Fig. 3. Typical type 2 Cu ('normal Cu', square planar coordination) signals with hyperfine coupling ($g_{\parallel} \approx 2.215$, $A_{\parallel} \approx 594$ MHz) were observed for all the samples, as well as seven hyperfine peaks ranging from 318.4 to 329.7 mT, with hyperfine splitting around 14–15 G. The first derivative spectrum was taken, and although the spectrum deviated somewhat from the expected theoretical intensity pattern, 1:3:6:7:6:3:1, the number of peaks (seven) indicates that there could be three ^{14}N coordinated with Cu(II) sites in both MnxEF and the MnxEF3 mutant. This finding indicates that the Cu ligands are not the conserved His residues in MnxF that were mutated to Ala.

The lowest Cu binding stoichiometry MnxEF3 sample (0.26 Cu:EF3) was selected for one component simulation of a single T2 Cu, which assumed that Cu is tightly bound to three ^{14}N -containing ligands (Fig. 3B). Axial Cu(II) parameters were obtained from the simulation, which was named "Cu species 1", with $g_{\parallel} \approx 2.215$, $A_{\parallel} \approx 594$ MHz and $g_{\perp} \approx 2.052$, $A_{\perp} \approx 72$ MHz; as well as $A_{\parallel} \approx 42$ MHz and $A_{\perp} \approx 45$ MHz for ^{14}N hyperfine. However, this simulation is not sufficient to accurately model the rest of the higher Cu stoichiometry MnxEF spectra. Rather, a two-component simulation involving a second, distinct, type 2 Cu was needed, suggesting that a second Cu binding site besides the one with three ^{14}N is coordinated in the MnxEF subunits. The relative contributions of "Cu species 2" and "Cu species 1" to the spectra of the differentially Cu loaded samples were simulated (Fig. 4, Table 1). Overall, there appears to be a tendency for the protein bind more Cu species 1 than Cu species 2, especially the MnxEF3 mutant.

Having established that a N-coordinated type 2 Cu signal was present within the MnxEF complex, Cu(I) K-edge XAS was used to determine whether the interatomic distances observed were consistent with N binding from His residues, which would produce an unmistakable multiple scattering contribution, or from amide species from other peptide or backbone residues. wtMnxEF with a Cu to protein ratio of 3:1 was concentrated to 3 mM and reduced with dithionite before loading in the XAS sample cuvette. The simulation of the Cu K-edge EXAFS was straightforward, with a best fit that included multiple scattering nitrogen and carbon contributions from three histidines at ~ 1.97 Å (Fig. 5). Importantly, the Debye-Waller (DW) factor for the simulation was equal for all three histidines at a relatively low 0.010 Å 2 despite attempting to find unique DW values by treating the histidines as individual shells, indicating that the histidines are equivalent in their binding contributions to Cu(I). An attempt to add a fourth histidine ligand resulted in a slight increase in the fit index (from 0.37 to 0.62), and a slight increase in the DW (from 0.010 to 0.015 Å 2), which we interpret as the possibility of a fourth histidine residue. The fit to a Cu coordinated by histidines is consistent with the EPR data. As the XAS likely shows an average of all binding sites, and may indicate that the MnxEF complex contains one or more type 2 Cu binding sites, each of which contains a unique number of histidine ligands of the eleven available.

4. Discussion

MCOs are thought to be one of the main drivers of Mn cycling in the environment because bacteria use them and peroxidases to catalyze Mn oxidation. Reduced Mn species are stable in oxic terrestrial and aquatic environments: Mn(II) is inherently stable and Mn(III) is stabilized by naturally occurring ligands [25]. However, Mn(IV) is a potent oxidant, and is able to catalyze the oxidation several of other metals and the degradation of organics, like herbicides, pesticides, and humic substances

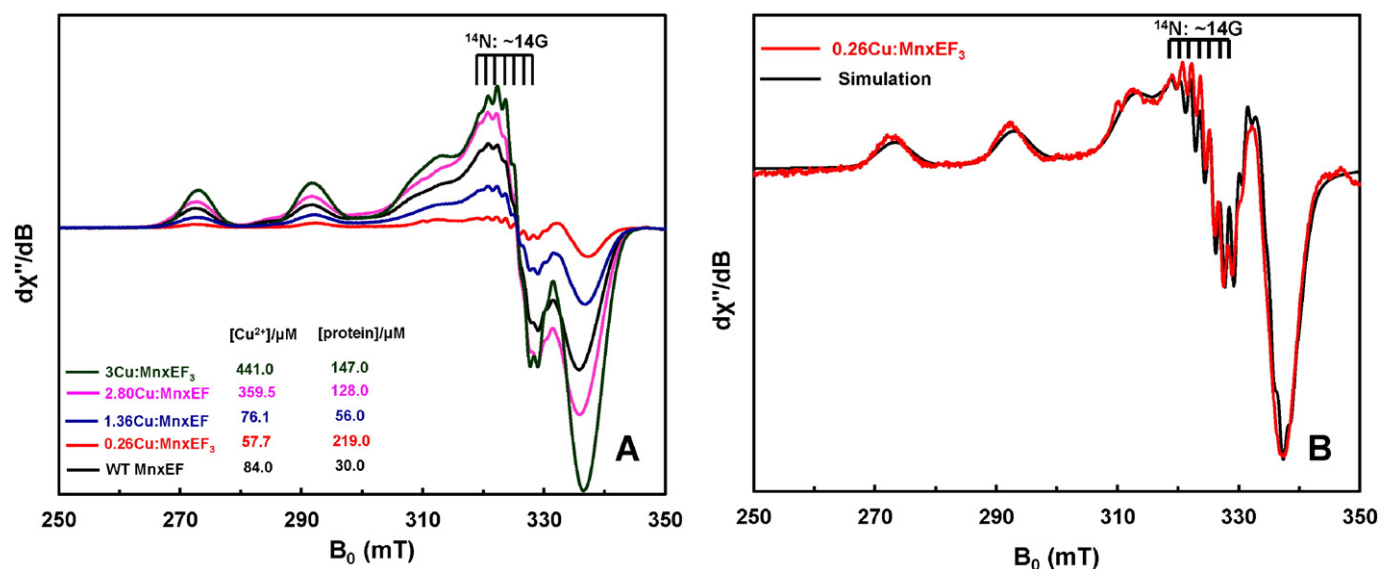


Fig. 3. Comparison of samples by EPR. (A) X-band CW EPR spectra of a set of both wtEF and triple H21/80/82A mutant EF3 samples with varying Cu stoichiometry. The samples were analyzed at 40 K and 0.02 mW power. Parameters: microwave frequency: 9.38 GHz, conversion time: 40 ms, modulation amplitude: 8 G, and modulation frequency: 100 kHz. (B) X-band CW EPR spectra of 0.26 Cu:EF3 mutant as well as simulation (also referred to as Cu species 1). Nucleus: “Cu, ¹⁴N, ¹⁴N, ¹⁴N”; $g = [2.052, 2.052, 2.215]$, $A_{Cu} = [72, 72, 594]$ MHz and $A_{N} = [42, 42, 45]$ MHz.

[29]. Oxidation of recalcitrant species by Mn(IV) would then contribute to the global carbon cycle by potentially releasing low molecular weight organics to feed bacteria. To overcome the kinetic barrier of Mn(II) oxidation, bacteria evolved enzymes to directly oxidize Mn(II, III) to Mn(IV), forming Mn-oxide minerals. These Mn-oxide minerals coat the outermost layer of the bacteria and provide a physical shield between the cell and the environment, which may help the cell avoid predation and UV irradiation [24]. While the physiological purpose of bacterial Mn oxidation remains unclear, elucidating the mechanism is central to understanding this fundamental biogeochemical process.

The Mnx system is the first known multicopper oxidase to require the presence of accessory proteins, which prioritizes the elucidation of their characterization and function. In particular, determining the role of each unit of the Mnx complex will likely prove to be important for determining the structure–function relationship of electron transfer and the substrate turnover mechanism. We previously observed that MnxE and MnxF accompany MnxG in an uncertain stoichiometry within the Mnx complex, and now it is apparent that oligomerization is not contingent on the presence of MnxG. While the exact stoichiometry of MnxE and MnxF subunits relative to each other in the oligomer is still unknown, we posit that there are at least six ~12 kDa subunits in the Mnx complex based on the calculated size of the purified MnxEF oligomer. More sophisticated structural analyses like top-down, whole protein mass spectrometry and ultra-centrifugation will be employed to probe further into the question of subunit stoichiometry in Mnx.

Sequence homology and spectroscopy were used to investigate Cu binding within the small Mnx subunits. We observed that three available MnxE and MnxF sequences contain zero conserved methionines, two conserved cysteines, and three conserved histidine residues that could contribute to Cu binding like those found in MnxG. However, mutating the three conserved His to Ala showed that they are not involved Cu binding within the EF hexamer. Mutagenesis of the other eight *Bacillus* sp. PL-12 MnxE and MnxF His residues will be needed.

Quantifying the exact number of bound Cu atoms in the Mnx system has been challenging, but we find that the MnxEFG complex binds between 6–15 atoms of Cu per 230 kDa protein complex depending on preparation schemes and dialysis buffer [14,17]. Starting with the assumption that MnxG, an MCO, should bind four Cu, we expect MnxEF to bind the remaining Cu. Puzzlingly, the purified MnxEF hexamer

only binds three Cu based on oxidation-independent quantification analysis. With three Cu in MnxEF and four Cu in MnxG, the remaining three may bind when the subunits come together to form the MnxEFG protein complex.

The spectroscopic analyses undertaken in these experiments have resulted in the assignment of one type 2 center coordinated by histidines and another, as yet unresolved Cu²⁺ species. The EPR simulations suggest the presence of two Cu binding centers with distinct spectroscopic characteristics. Under-loading the MnxEF triple mutant protein with Cu resulted in a simple spectrum that can be simulated with one component, termed “Cu species 1”. “Cu species 1” binds Cu with three N ligands from imidazole. We compared this simulation to the fully loaded triple mutant and wild type protein spectra and we found that while all samples have this feature, there was another common contribution to the spectra. This feature, termed “Cu species 2”, also contains type 2 Cu, based on the EPR simulations, but lacks the well-resolved ¹⁴N hyperfine seen in species 1. Based on the presence of “Cu species 1” in the under-loaded sample, we propose that “Cu species 1” has higher affinity than “Cu species 2”. Unfortunately, due to the lack of resolved hyperfine coupling in the EPR spectra we cannot describe the nature of this binding with the current data. The Cu K-edge EXAFS is consistent with the EPR analysis; 3 to 4 N(His) shells could be fit to the MnxEF mixture, with reasonable Debye–Waller factors and quality of fit for both scenarios. Taking both approaches together, we can assign an axial symmetry with 3 His ligands to “Cu species 1”, which is probably a somewhat distorted 4-coordinate or perhaps tetragonal 5-coordinate site with an axial water.

We were surprised to find that affinity-purified MnxEF appears to specifically bind heme. The low-spin spectrum of the MnxEF complex (oxidized: 412, 535, and 565 nm; reduced: 425, 538, 560 nm) implies that the heme is bound by two axial ligands, and the peaks lie well within the literature values for other heme proteins like mammalian cytochrome *b*₅ (His/His Fe axial coordination) (oxidized: 410 nm; reduced: 423, 527, and 555 nm) [30] and a heme peroxidase from *Streptomyces refuineus* (oxidized: 408, 530, and 561 nm) [31]. Both wild type and triple mutant MnxEF bind 0.38 and 0.36 heme per hexamer, respectively. Higher loading stoichiometry may be achieved with an in vivo technique as we have observed in the case for Cu and Mnx. While adventitious high-spin Fe-heme binding to apolar solvent-exposed residues has been described in proteins like serum

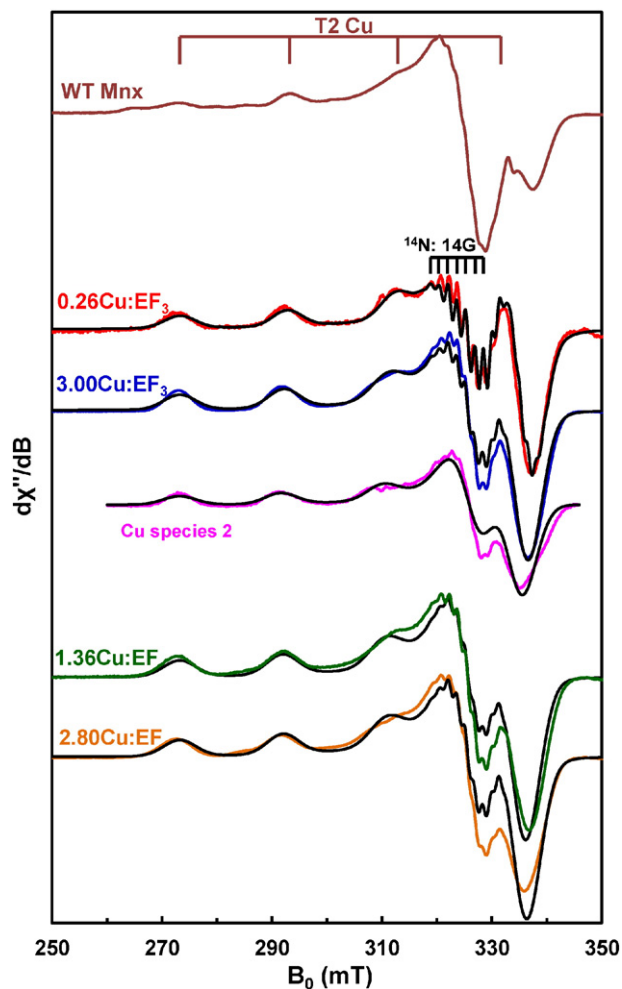


Fig. 4. X-band CW EPR spectra of WT MnxEFG complex (top brown), triple H21/80/82A mutant EF₃ samples and WT MnxEF samples with varying Cu stoichiometry. The samples were analyzed at 40 K and 0.2 mW power. Parameters: microwave frequency: 9.38 GHz, conversion time: 40 ms, modulation amplitude: 8 G, and modulation frequency: 100 kHz. Two-component simulations are shown in black traces for both MnxEF₃ mutants and WT MnxEF. The first component (Cu species 1) is based on hypothesizing that only one Cu species presented in sub-stoichiometry “0.26 Cu:EF₃” sample, with simulation parameters as the following: Nucleus: “Cu, ¹⁴N, ¹⁴N, ¹⁴N”; $g = [2.052, 2.052, 2.215]$, $A_{Cu} = [72, 72, 594]$ MHz and $A^{14N} = [42, 42, 45]$ MHz. The second component (Cu species 2) is based on the spectrum (purple) obtained by subtracting the spectrum of “0.26 Cu:EF₃” from that of “3.00 Cu:EF₃”, with simulation parameters as the following: Nucleus: “Cu”; $g = [2.054, 2.054, 2.228]$, and $A_{Cu} = [30, 30, 564]$ MHz. The distributions of two component Cu species are shown in Table 1.

albumin (in the absence of substrate), we believe MnxEF could specifically bind heme with any combination of the two S(Cys), six S(Met), and eight N(His) because apo-protein purification resulted in the partial heme loading of the protein, possibly indicating high heme affinity [32–34].

Table 1

Distributions of two binding Cu(II) species in both wtEF and triple H21/80/82A mutant EF₃ samples with varying Cu stoichiometry based on simulations.

Sample	[Protein] (μM)	[Cu ²⁺] (μM)	Ratio of Cu/protein	[Cu ²⁺ species 1] (%) ^a	[Cu ²⁺ species 2] (%) ^b
0.26 Cu:MnxEF ₃	219	57.8	0.26	100	0
3.00 Cu:MnxEF ₃	147	441	3.00	61.6 ± 1	38.4 ± 1
1.36 Cu:MnxEF	56.0	76.1	1.36	60.7 ± 10	39.3 ± 10
2.80 Cu:MnxEF	128	359	2.80	48.3 ± 5	51.7 ± 5

^a With simulation parameters as the following: Nucleus: “Cu, ¹⁴N, ¹⁴N, ¹⁴N”; $g = [2.052, 2.052, 2.215]$, $A_{Cu} = [72, 72, 594]$ MHz and $A^{14N} = [42, 42, 45]$ MHz.

^b With simulation parameters as the following: Nucleus: “Cu”; $g = [2.054, 2.054, 2.228]$, and $A_{Cu} = [30, 30, 564]$ MHz.

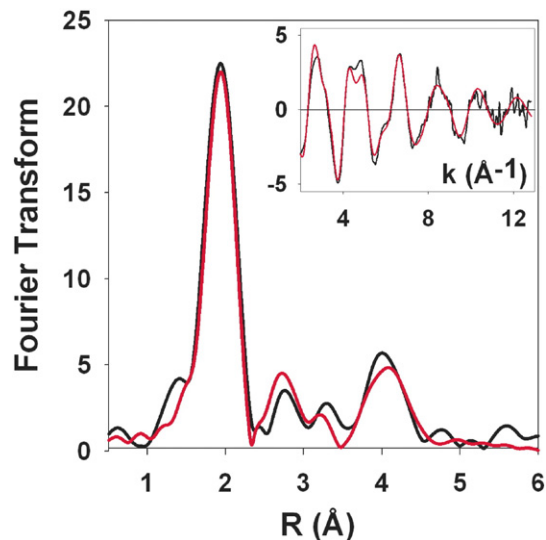


Fig. 5. Experimental and simulated Fourier Transforms and EXAFS (inset) for Cu(I)-loaded MnxEF. The experimental data (black) agrees well with the simulation (red) of Cu binding to three multiple scattering N(His) ligands at ~ 1.97 Å, with a Debye–Waller of 0.010 Å², an E_0 of -4.621 , and a fit index of 0.037 .

The combined presence of histidine-ligated Cu and heme is unexpected in this system. It is possible that a parallel to heme/Cu protein cytochrome c oxidase may be drawn from these results. Cytochrome c oxidase contains a Cu_B site, which together with heme *a* forms the catalytic site for oxygen reduction. Cu_B is known to be a type 2 Cu with square planar geometry comprised of three equivalent N(His) ($g_{\parallel} 2.20$, $A_{\parallel} 190$ G and $g_{\perp} 2.06$), which is similar to values found in MnxEF ($g_{\parallel} 2.215$, $A_{\parallel} 191.5$ G and $g_{\perp} 2.052$) [35]. The negative shift in the Cu g values in the assembled MnxEFG complex brings the spectroscopic features even closer to what is found in Cu_B. This negative shift could then be indicative of a shift in geometry that primes the site for catalysis. An analogous heme/Cu center in MnxEF would be of deep interest, as examples are rare in the literature, particularly outside the context of terminal oxidases. Unfortunately, the heme loading experiments were performed after the Cu spectroscopy so we were not able to evaluate if the two centers interact. Further research will determine whether structural and chemical similarities exist between MnxEF and cytochrome c oxidase to provide evidence for an O₂ binding site beyond the one located at the trinuclear Cu center of MnxG.

5. Conclusions

These experiments demonstrate that two types of Cu and a low-spin heme bind to MnxEF. It may not be a coincidence that the only MCO to carry out the two electron oxidation of a metallo-substrate is also the only MCO to require the co-expression of accessory proteins that contain redox active metal centers. The concurrence of these two features may suggest that MnxEF do play a role in Mn oxidation in Mnx. While

these data add to the complexity of the Mn oxidase complex and make determining a catalytic mechanism more difficult, the data gathered on this system disrupts the canonical view of a well-studied class of enzymes, the multicopper oxidases, for the environmentally significant biomineralizing agent, Mnx.

Transparency document

The Transparency document associated with this article can be found, in the online version.

Acknowledgments

We thank Larry David and John Klimek at the Oregon Health & Science University Proteomics Shared Resource for analyzing the protein samples, Alison Tebo for thoughtful comments during the preparation of this manuscript and Prof. Leone Spiccia of Monash University for discussions. Funding for this work was provided by the National Science Foundation, Chemistry of Life Processes Program grants CHE-1410688 to BMT and CHE-1410353 to TGS and a Geobiology and Low Temperature Geochemistry program grant EAR1231322 to WHC. Portions of this research were carried out at the SSRL, a Directorate of Stanford Linear Accelerator Center National Accelerator Laboratory and an Office of Science User Facility operated for the US Department of Energy Office of Science by Stanford University.

Appendix A. Supplementary data

Supplementary data to this article can be found online at <http://dx.doi.org/10.1016/j.bbapap.2015.08.012>.

References

- [1] J. Chatt, J.R. Dilworth, R.L. Richards, J.R. Sanders, Chemical evidence concerning the function of molybdenum in nitrogenase [13], *Nature* 224 (1969) 1201–1202.
- [2] J. Kim, D.C. Rees, Structural models for the metal centers in the nitrogenase molybdenum–iron protein, *Science* 257 (1992) 1677–1682.
- [3] G. Nakos, L. Mortenson, Molecular weight and subunit structure of molybdoferredoxin from *Clostridium pasteurianum* W5, *Biochim. Biophys. Acta Protein Struct.* 229 (1971) 431–436.
- [4] C. Kisker, H. Schindelin, B.E. Alber, J.G. Ferry, D.C. Rees, A left-handed β -helix revealed by the crystal structure of a carbonic anhydrase from the archaeon *Methanosarcina thermophila*, *EMBO J.* 15 (1996) 2323–2330.
- [5] K.S. Smith, J.G. Ferry, A plant-type (β -class) carbonic anhydrase in the thermophilic methanoeocyte *Methanobacterium thermoautotrophicum*, *J. Bacteriol.* 181 (1999) 6247–6253.
- [6] R. Lehneck, P. Neumann, D. Vullo, S. Elleuche, C.T. Supuran, R. Ficner, S. Pöggeler, Crystal structures of two tetrameric β -carbonic anhydrases from the filamentous ascomycete *Sordaria macrospora*, *FEBS J.* 281 (2014) 1759–1772.
- [7] M.A. Culpepper, A.C. Rosenzweig, Architecture and active site of particulate methane monooxygenase, *Crit. Rev. Biochem. Mol. Biol.* 47 (2012) 483–492.
- [8] T.J. Lawton, J. Ham, T. Sun, A.C. Rosenzweig, Structural conservation of the B subunit in the ammonia monooxygenase/particulate methane monooxygenase superfamily, *Proteins: Struct., Funct., Bioinf.* 82 (2014) 2263–2267.
- [9] P. Reichard, Ribonucleotide reductases: substrate specificity by allostery, *Biochem. Biophys. Res. Commun.* 396 (2010) 19–23.
- [10] H. Michel, J. Behr, A. Harrenga, A. Kann, Cytochrome C oxidase: structure and spectroscopy, *Annu. Rev. Biophys. Biomol. Struct.* 27 (1998) 329–356.
- [11] E.I. Solomon, U.M. Sundaram, T.E. Machonkin, Multicopper oxidases and oxygenases, *Chem. Rev.* 96 (1996) 2563–2605.
- [12] E.I. Solomon, D.E. Heppner, E.M. Johnston, J.W. Ginsbach, J. Cirera, M. Qayyum, M.T. Kieber-Emmons, C.H. Kjaergaard, R.G. Hadt, L. Tian, Copper active sites in biology, *Chem. Rev.* 114 (2014) 3659–3853.
- [13] C.S. Stoj, A.J. Augustine, L. Zeigler, E.I. Solomon, D.J. Kosman, Structural basis of the ferrous iron specificity of the yeast ferroxidase, Fet3p, *Biochemistry* 45 (2006) 12741–12749.
- [14] C.N. Butterfield, A.V. Soldatova, S.W. Lee, T.G. Spiro, B.M. Tebo, Mn(II, III) oxidation and MnO₂ mineralization by an expressed bacterial multicopper oxidase, *Proc. Natl. Acad. Sci. U. S. A.* 110 (2013) 11731–11735.
- [15] C.A. Francis, K.L. Casciotti, B.M. Tebo, Localization of Mn(II)-oxidizing activity and the putative multicopper oxidase, MnxG, to the exosporium of the marine *Bacillus* sp. strain SG-1, *Arch. Microbiol.* 178 (2002) 450–456.
- [16] G.J. Dick, J.W. Torpey, T.J. Beveridge, B.M. Tebo, Direct identification of a bacterial manganese(II) oxidase, the multicopper oxidase MnxG, from spores of several different marine *Bacillus* species, *Appl. Environ. Microbiol.* 74 (2008) 1527–1534.
- [17] C.N. Butterfield, Characterizing the Mn(II) Oxidizing Enzyme From the Marine *Bacillus* sp. PL-12 Spore, *Environmental and Biomolecular Systems*, Oregon Health & Science University, Portland, OR, 2014 102.
- [18] R. Edgar, MUSCLE: a multiple sequence alignment method with reduced time and space complexity, *BMC Bioinf.* 5 (2004) 1–19.
- [19] R.C. Edgar, MUSCLE: multiple sequence alignment with high accuracy and high throughput, *Nucleic Acids Res.* 32 (2004) 1792–1797.
- [20] P. Durão, Z. Chen, A.T. Fernandes, P. Hildebrandt, D.H. Murgida, S. Todorovic, M.M. Pereira, E.P. Melo, L.O. Martins, Copper incorporation into recombinant CotA laccase from *Bacillus subtilis*: characterization of fully copper loaded enzymes, *J. Biol. Inorg. Chem.* 13 (2008) 183–193.
- [21] S. Stoll, A. Schweiger, EasySpin, a comprehensive software package for spectral simulation and analysis in EPR, *J. Magn. Reson.* 178 (2006) 42–55.
- [22] G.N. George, (1995).
- [23] S.J. Gurman, N. Binsted, I. Ross, A rapid, exact curved-wave theory for EXAFS calculations, *J. Phys. C Solid State Phys.* 17 (1984) 143–151.
- [24] K. Geszvain, C. Butterfield, R. Davis, A. Madison, S. Lee, D. Parker, A. Soldatova, T. Spiro, G. Luther, B. Tebo, The molecular biogeochemistry of manganese (II) oxidation, *Biochem. Soc. Trans.* 40 (2012) 1244.
- [25] R.E. Trouwborst, B.G. Clement, B.M. Tebo, B.T. Glazer, G.W. Luther 3rd, Soluble Mn(III) in suboxic zones, *Science* 313 (2006) 1955–1957.
- [26] L. Basumallick, R. Sarangi, S. DeBeer George, B. Elmore, A.B. Hooper, B. Hedman, K.O. Hodgson, E.I. Solomon, Spectroscopic and density functional studies of the red copper site in nitrosocyanin: role of the protein in determining active site geometric and electronic structure, *J. Am. Chem. Soc.* 127 (2005) 3531–3544.
- [27] D.M. Arciero, B.S. Pierce, M.P. Hendrich, A.B. Hooper, Nitrosocyanin, a red cupredoxin-like protein from *Nitrosomonas europaea*, *Biochemistry* 41 (2002) 1703–1709.
- [28] T. Yonetani, H. Anni, Yeast cytochrome c peroxidase. Coordination and spin states of heme prosthetic group, *J. Biol. Chem.* 262 (1987) 9547–9554.
- [29] T.G. Spiro, J.R. Bargar, G. Sposito, B.M. Tebo, Bacteriogenic manganese oxides, *Acc. Chem. Res.* 43 (2010) 2–9.
- [30] S. Beck von Bodman, M.A. Schuler, D.R. Jollie, S.G. Sligar, Synthesis, bacterial expression, and mutagenesis of the gene coding for mammalian cytochrome b5, *Proc. Natl. Acad. Sci. U. S. A.* 83 (1986) 9443–9447.
- [31] K.L. Connor, K.L. Colabroy, B. Gerratana, A heme peroxidase with a functional role as an L-tyrosine hydroxylase in the biosynthesis of anthracycline, *Biochemistry* 50 (2011) 8926–8936.
- [32] G.H. Beaven, C. Shi Hua, A. D'Albis, W.B. Gratzner, A spectroscopic study of the haemin human serum albumin system, *Eur. J. Biochem.* 41 (1974) 539–546.
- [33] P. Ascenzi, M. Fasano, Serum heme–albumin: an allosteric protein, *IUBMB Life* 61 (2009) 1118–1122.
- [34] C. Meneghini, L. Leboffe, M. Bionducci, G. Fanali, M. Meli, G. Colombo, M. Fasano, P. Ascenzi, S. Mobilio, The five-to-six-coordination transition of ferric human serum heme–albumin is allosterically-modulated by ibuprofen and warfarin: a combined XAS and MD study, *PLoS One* 9 (2014) e104231.
- [35] A. Pezeshk, J. Torres, M.T. Wilson, M.C.R. Symons, The EPR spectrum for CuB in cytochrome c oxidase, *J. Inorg. Biochem.* 83 (2001) 115–119.